Optics Communications 283 (2010) 1138–1143

Contents lists available at ScienceDirect

Optics Communications

journal homepage: www.elsevier.com/locate/optcom

# Broadband non-collinear double QPM optical parametric amplification in mid-infrared wave

Shi Yong Feng, Zhang Wei Quan *, Yang Fan, Li Xiao Yun

*Department of Physics, Zhejiang Sci-Tech University, Key Laboratory of Advanced Textile Materials and Manufacturing Technology Ministry of Education, Hanghou, Zhejiang 310018, China*

ARTICLE INFO

*Article history:*
Received 10 April 2009
Received in revised form 18 October 2009
Accepted 3 November 2009

*Keywords:*
Broadband double quasi-phase matching
Gain bandwidth
Spatial–temporal frequency band

ABSTRACT

The properties of optical parametric amplification (OPA) based on non-collinear double quasi-phase matching (NDQPM) with single periodically poled KTP (PPKTP) have been investigated theoretically. The NDQPM includes two different non-linear processes: one is optical parametric generation (OPG) and the other is difference frequency generation (DFG). The investigation of our numerical simulation focuses on the gain bandwidth of dependence upon non-collinear angle, grating period and crystal temperature. At a certain non-collinear angle and grating period with fixed temperature, there exists a broadest gain bandwidths of output mid-infrared pulse at 526 nm pump wavelength and certain signal wavelength in PPKTP. These are an optimal values of non-collinear angles and grating period. By accurately tuning the non-collinear angle or temperature near the optimal non-collinear angle, broadband mid-infrared tuning is obtained and an optimal operation of NDQPM can be realized. In this paper, the solutions of the coupled equations of the cascaded processes were discussed, and the spatial–temporal frequency (STF) band of the output idler pulse is analyzed by taking angular dispersion of amplified pulse beam into account. The idler pulse with a certain angular dispersion can improve the OPA bandwidth significantly. So, optical parametric chirped-pulse amplification can be realized in this configuration. For a broadband NDQPM both the acceptance angles and the acceptance temperature are smaller and the gain bandwidth is sensitive to non-collinear angles and temperature, it is important to control the precision of the non-collinear angles and the temperature in experiment.



## 1. Introduction

Quasi-phase matching (QPM) materials can improve parametric gain properties. First, the highest effective non-linear coefficients could be realized through QPM technology. Second, it eliminates the limitation on the interaction length associated with spatial walk-off. Further, broad bandwidth gain in OPA can be realized in non-collinear geometry [1]. Recently, broadband amplifications of mid-infrared OPA with significant optical gain have been achieved in non-collinear and near-collinear geometry using PPKTP [2–4]. The broadband optical parametric amplification can obtain tunable mid-infrared ultrashort pulse. Broadband degenerate optical parametric generator with PPKTP has been investigated by Thhonen et al. [5]. In the device the group velocities are approximately matched and the group-velocity dispersions (GVD) are very small. Application of optical parametric amplification to chirped-pulse amplification was defined as optical parametric chirped-pulse amplification (OPCPA) [6–8]. This attractive technique has been applied to amplification of ultrashort pulses for high power output. The technology has many advantages, such as high gain with broad bandwidth, high signal-to-noise contrast ratio.

To achieve tunable mid-infrared output, two separated periodically-poled crystals were used within the resonator, in which independent temperature phase matching of both OPG and DFG processes is allowed [9–13]. The mid-infrared sources can also be generated through several non-linear processes using a resonant cavity and a single periodically-poled crystal in a collinear interaction [14,15], but this configuration prevents tuning ability because the unique phase-matching conditions must meet for two processes, which occurred within the same crystal at a single temperature. Using a non-collinear interaction provides another degree of freedom that can be used, together with the QPM period, for phase matching simultaneously two different interactions. Furthermore, in a non-collinear configuration, the double quasi-phase matching conditions can be satisfied over a broad spectral range in single periodically-poled crystal [16]. Zhang has investigated the non-collinear double quasi-phase matching theoretically [17]. This type of poled structure can generate OPG and DFG in single grating, simultaneously.

* Corresponding author.
*E-mail address:* mike@hosonic.com.cn (W.Q. Zhang).

0030-4018/$ - see front matter © 2009 Elsevier B.V. All rights reserved.
doi:10.1016/j.optcom.2009.11.023

In chirped pulse optical parametric amplifiers, the group-velocity dispersion and diffraction cause the spreading of pulse beam in time and space, respectively. The group velocity, non-collinear angles and linear angular spectral dispersion coefficients of signal and idler waves should be suitably linked to each other for ultra-broadband three-wave mixing. A broadband amplification of angularly dispersed signal requires matching of an angular spectrum of a signal pulse with an acceptance angle of OPA. So, the spatial–temporal frequency band of OPA should be considered [18].

The purpose of this paper is to explore a broadband mid-infrared OPA using cascaded downconversion process with single PPKTP. First, we investigate the dependence of gain bandwidth and the corresponding grating period on the non-collinear angle with the signal pulse of certain wavelength. Selecting the proper grating period and non-collinear angles, broadband mid-infrared optical parametric amplification can have a good performance under a fixed temperature. Second, temperature tuning at the optimal non-collinear angles and the corresponding grating period were also discussed. A broadband OPA of angle tuning and temperature tuning can be obtained. Third, the solution of coupled equation in NDQPM and the spatial–temporal frequency band of the output idler pulse were analyzed. Because the gain bandwidths of output idler and mid-infrared pulses are very large and spectrum dispersion is matched with angular dispersion, an OPCPA can be realized at wider wavelength range by NDQPM.

## 2. Double quasi-phase matching and gain bandwidth

For double phase matching processes, the conditions of energy conservation are, respectively

$$\omega_p = \omega_s + \omega_i \quad \text{(for OPG)},$$

$$\omega_s = \omega_i + \omega_M \quad \text{(for DFG)}, \tag{1}$$

where the subscripts $p$, $s$, $i$ and $M$ represent pump, signal, idler and mid-infrared waves, respectively. For a non-collinear geometry with 1D phase-matching condition in periodic QPM grating, waves propagate in the $y$–$z$ plane, perpendicular to the crystallographic $b$-axis. From the NDQPM geometrical consideration, the conditions of momentum conservation of both OPG and DFG processes are shown as following [17]:

$$\mathbf{\Delta K} = \mathbf{K_p} - \mathbf{K_s} - \mathbf{K_i} - \mathbf{G} = 0 \quad \text{(for OPG)},$$

$$K_s^2 + (K_i + K_M)^2 - 2K_s(K_i + K_M)\cos(\theta_s - \theta_i) = G^2 \quad \text{(for DFG)}. \tag{2}$$

For OPG process, the components of the wave-vector mismatch $\mathbf{\Delta K}$ parallel and perpendicular to the grating vector $\mathbf{G}$ are, respectively

$$K_\parallel = K_p \cos\theta_p - K_s \cos\theta_s - K_i \cos\theta_i - G, \tag{3}$$
$$K_\perp = K_p \sin\theta_p - K_s \sin\theta_s - K_i \sin\theta_i, \tag{4}$$

where $\theta_p$, $\theta_s$, and $\theta_i$ angles are non-collinear angles of $\mathbf{K_p}$, $\mathbf{K_s}$ and $\mathbf{K_i}$ with respect to the grating vector, respectively.

Such non-collinear double interaction in a tilted QPM grating is described by two kinds of the wave vector geometry: assume that all wave vectors lie in same meridian plane, their direction cosines are, respectively,

$$K_{yj} = \sin(\xi - \theta_j), \quad k_{zj} = \cos(\xi - \theta_j) \tag{5}$$

or

$$k_{yj} = \sin(\xi + \theta_j), \quad k_{zj} = \cos(\xi + \theta_j) \quad (j = p, s, i \text{ or } M), \tag{6}$$

where $\xi$ denotes the angle between $\mathbf{G}$ and $\mathbf{z}$-axis. With reference to Fig. 1a and b, Eq. (5) corresponds to counterclockwise angles with respect to $z$-axis and Eq. (6) to clockwise angles. In these figs. wave-vector $K_j = 2\pi\, n_j/\lambda_j$ ($j = p, s, i$ or $M$) and the calculation of the refractive indices $n_j$ was given in Ref. [19]. In the calculation, according to convention, $n_x < n_y < n_z$ are satisfied and Sellmeier expansions was given in Ref. [20]. $G = 2\pi/\Lambda$ and $\Lambda$ is the grating period. Selecting proper grating period and non-collinear angles, for certain pump wavelength the phase-matching conditions Eq. (2) of both OPG and DFG processes can be satisfied, simultaneously. The DNQPM is realized.

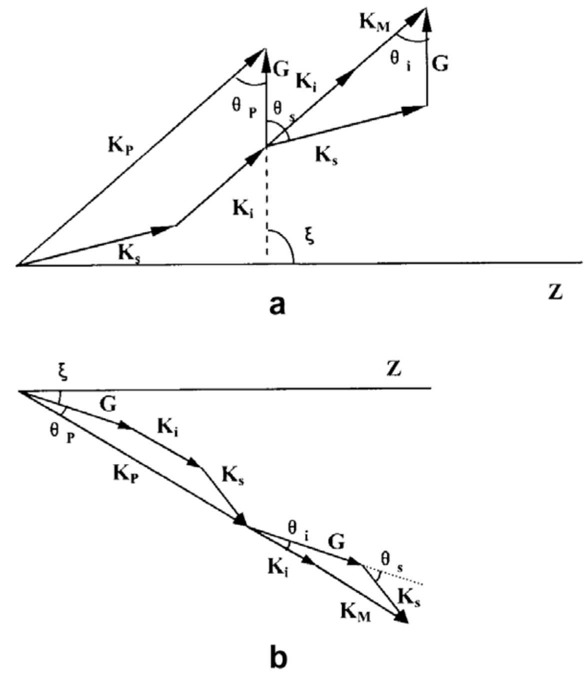


**Fig. 1.** Wave vectors of non-collinear double quasi-phase matched waves: (a) counterclockwise angles with respect to **z** axis $\theta = \xi - \theta_j$; and (b) the clockwise angles $\theta = \xi + \theta_j$.

The relative parametric gain $G$ is given by [21]

$$G = \mathrm{Sinc}^2\{[(\Delta K/2)2 - \Gamma^2]^{1/2} L\}, \tag{7}$$

where $L$ is interaction length in the crystal and

$$\Gamma = 4\pi|E_p|d_{\mathrm{nm}}(/n_p n_s n_i \lambda_s \lambda_i)^{1/2} \quad \text{(for OPG)}$$

or

$$\Gamma = 4\pi|E_s|d_{\mathrm{nm}}/(n_s n_i n_M \lambda_i \lambda_M)^{1/2} \quad \text{(for DFG)}, \tag{8}$$

where $d_{\mathrm{nm}} = d_{\mathrm{eff}}\, g_m$ can be defined as the effective non-linear coefficients, and $g_m$ is the amplitude of the reciprocal vector $\mathbf{G}$ of periodically-poled crystal [22]. $E_s$ and $E_p$ are the electric field intensities of the incident light for both processes, respectively. $\Delta K$ are the wave-vector mismatching. The gain bandwidth determined by the first-order term in the expanding expression of wave vector mismatched is [17]

$$\Delta\lambda = 2[(1.392/L)^2 + \Gamma^2]^{1/2}/[d\Delta K/d\lambda|_{\lambda 0}], \tag{9}$$

where $\lambda_0$ are the wavelength of perfect phase matched. If the first-order term vanishes, the gain bandwidth is limited by the second-order term. The gain bandwidth is given by

$$\Delta\lambda = \{4[(1.392/L)^2 + \Gamma^2]1/2/[d^2\Delta K/d\lambda 2|_{\lambda 0}]\}^{1/2}, \tag{10}$$

$d\,\Delta K/d\lambda$ and $d^2\Delta K/d\lambda^2$ have be calculated in Ref. [17]. Above formulas give calculations of phase-matching conditions and gain bandwidth for NDQPM at two kinds of the wave vector geometry.

## 3. Non-collinear angle tuning

Based on above expressions, the gain bandwidth of dependence upon several factors such as grating period $\Lambda$, non-collinear angle $\theta_s$ and crystal temperature $T$ was analyzed. A series of optimal values which correspond to maximal gain bandwidth were got by numerical simulations. The parameters are given as following: The pump wavelength is 526 nm, length of PPKTP is 10 mm. Here, we discuss the gain bandwidths $\Delta\lambda_M$ of mid-infrared wave and the grating period with the change of non-collinear angle at fixed temperature 25 °C in the NDQPM condition of Fig. 1. The $d\Delta K/d\lambda$ can be calculated according to formulas (10) in Ref. [17]. As shown in Fig. 2, for different non-collinear angles both the grating period and gain bandwidth are calculated when NDQPM condition is satisfied. The Fig. 2a corresponds to wave vector geometry Fig. 1a and the signal wavelength is centered at 902.5 nm .With the increase of non-collinear angle $\theta_s$, the grating period decreases monotonously. The maximal gain bandwidth is achieved at non-collinear angle $\theta_s = 6.08°$, which is thought as the optimal non-collinear angle, with the corresponding grating period $\Lambda = 16.1$ μm. To make sure that the interaction length can be not limited, at crystal length 10 mm the width should be about 1.1 mm. The Fig. 2b corresponds to wave vector geometry Fig. 1b and the signal wavelength is centered at 903.2 nm. The maximal gain bandwidth is achieved at non-collinear angle $\theta_s = 1.86°$ with the corresponding grating period $\Lambda = 16.05$ μm. When non-collinear angle deviates from optimal non-collinear angle, the gain bandwidth reduces quickly. From these results we know that the gain bandwidth is sensitive to non-collinear angle and the corresponding grating period must be properly selected to get maximal gain bandwidth.

The Fig. 3 shows the gain bandwidth $\Delta\lambda_M$ as a function of mid-infrared wavelength $\lambda_M$. In the figures the dashed curves correspond to the gain bandwidth determined by the first-order term in wavevector mismatched expansion. Fig. 3a corresponds to $\Lambda = 16.1$ μm and wave vector geometry Fig. 1a, the non-collinear angle $\theta_s$ is near to 6.08° and the signal wavelength is centered at 902.5 nm. At $\lambda_M = 3000$–3200 nm the first-order term vanishes nearly. Fig. 3b corresponds to $\Lambda = 16.05$ μm and wave vector geometry Fig. 1b, the non-collinear angle $\theta_s$ is near to 1.86° and the signal wavelength is centered at 903.2 nm. At $\lambda_M = 2400$–2600 nm the first-order term vanishes nearly. In the Fig. 3 the solid curves correspond to the gain bandwidth determined by the second-order term. The phase matching bandwidths determined by second-order term are about 60 nm [17]. In most cases the first-order term in expansion is large with respect to the second-order term, the second-order term can be neglected, and consequently the gain bandwidth is very small. For OPG process the $d\Delta K/d\lambda$ can be calculated according to formulas (8) in Ref. [23]. The gain bandwidth $\Delta\lambda_i$ of idler is about 35 nm. Because the gain bandwidths of both processes are both greater, it can be guarantied that the output pulse will be broadened. The group velocity mismatching is $1/v_h - 1/v_j$($h, j$ are $s$, $i$ or $M$ light). The group-velocity dispersion is $\frac{d(1/v_j)}{d\omega_j}$. According to formulas (2) in Ref. [24] and Sellmeier expansion, GVM is about 0.01 fs/μm. The GVD is about 0.1 fs$^2$/μm (at $\lambda_s = 850$–900 nm). The GVM is zero nearly. Selecting different

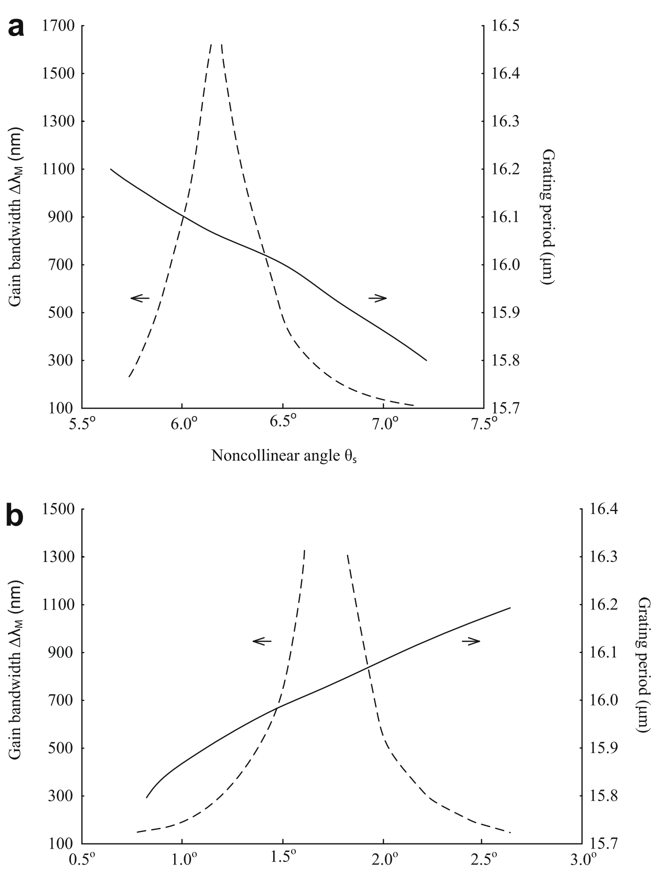


**Fig. 2.** Dependence of gain bandwidth and grating period upon non-collinear angle $\theta_s$ at $\lambda_p = 526$ nm, $T = 25$ °C and $L = 10$ mm; (a) for $\theta = \xi - \theta_j$ and signal central wavelength $\lambda_s = 902.5$ nm; and (b) for $\theta = \xi + \theta_j$ and $\lambda_s = 903.5$ nm.

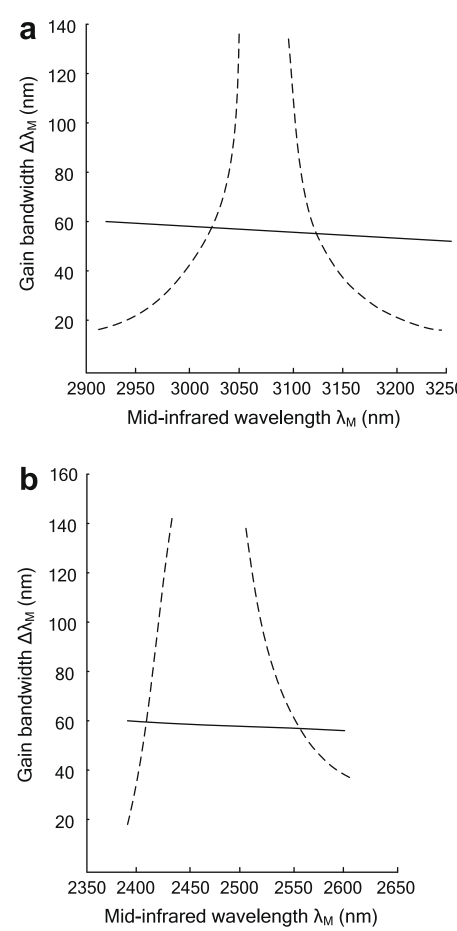


**Fig. 3.** Dependence of gain bandwidth $\Delta\lambda_M$ on $\lambda_M$; solid curve: the $\Delta\lambda_M$ determined by the second-order term; dashed curve: the $\Delta\lambda_M$ determined by the first-order term at the optimal grating period and near the optimal non-collinear angle, $L = 10$ mm; (a) for $\theta = \xi - \theta_j$ and $\Lambda = 16.1$ μm; and (b) for $\theta = \xi + \theta_j$ and $\Lambda = 16.05$ μm.

grating periods and the corresponding optimal non-collinear angles, broadband NDQPM optical parametric chirped-pulse amplification can be realized at different mid-infrared region. But the gain bandwidth is sensitive to non-collinear angle, so in experiment it is very important to keep the accurate non-collinear angle to get maximal gain bandwidth.

## 4. Temperature tuning

For a fixed non-collinear angle and grating period, NDQPM conditions can be met by changing the temperature at a certain range of signal, idler and mid-infrared frequencies. According to the thermo-optic dispersion formula in Ref. [20] and the thermal expansion formula in Ref. [25], the phase matching curves of temperature are shown in Fig. 4 with an optimal non-collinear angle $\theta_s$ and the corresponding grating period.

If temperature deviates from the idea phase matching temperature $T_0$, the phase mismatching is

$$\Delta K = |d\Delta K/dT|_{T0}|\Delta T.$$

For DFG process, from Fig. 1 we can obtain [17]

$$(K_i + K_M - \Delta K)^2 = K_s^2 + G^2 + 2K_s\, G\cos\theta_s. \tag{11}$$

We take the first order derivative of Eq. (11) with respect to $T$, given

$$\frac{d\Delta K}{dT} = \frac{dK_i}{dT} + \frac{dK_M}{dT} - \frac{dK_s/dT(K_s + G\cos\theta_s) + dG/dT(K_s\cos\theta_s + G)}{K_i + K_M}, \tag{12}$$

where $dK_j/dT = 2\pi/\lambda_j\,(dn_j/dT_j|_{T0})$. ($j = s$, $i$ or $M$) The calculations of $dn_j/dT_j$ are given in Ref. [13]. The acceptance temperature $\Delta T$ can be given by

$$\Delta T = 2[(1.392/L)^2 + \Gamma^2]^{1/2}/[d\Delta K/dT|_{T0}]. \tag{13}$$

The dependence of the acceptance temperature $\Delta T$ on crystal temperature $T$ is shown in Fig. 5. For $T = 30$ °C and $\theta = \xi + \theta_j$, $\Delta T$ is about 1.7 °C.

With the optimal grating period 16.07 μm, the phase matching crystal temperature and gain bandwidth with the change of non-collinear angle are shown in Fig. 6. In the figure the solid curve represents the phase matching temperature; the dashed curve represents the gain bandwidth. At the beginning the non-collinear angle increases with the increase of temperature; after it achieves idea non-collinear matching angle ($\theta_s$ is about 6.16°) in which the gain bandwidth reaches maximal, the non-collinear angle decreases with the increase of temperature. When the non-collinear angle deviates from idea non-collinear matching angle, the gain bandwidth reduces quickly. Selecting different grating period and the corresponding optimal non-collinear angle, a broadband NDQPM can be realized through tuning crystal temperature at different wavelength range. Since the acceptance temperature is vary small to keep larger gain bandwidth, it is important to control the precision of crystal temperature in experiment. The requirement is also proved in Ref. [26].

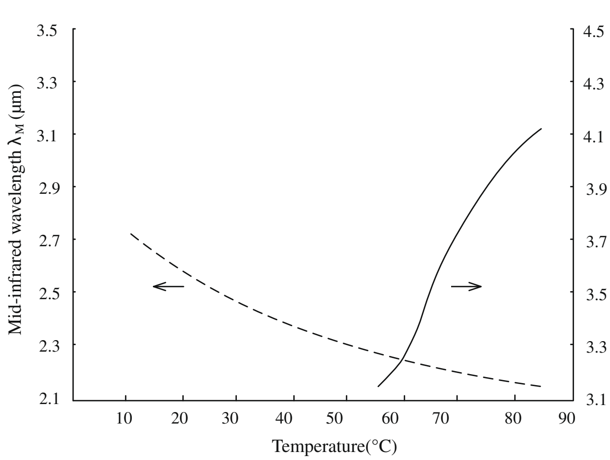


**Fig. 4.** Temperature tuning curve. Solid curves: for $\theta = \xi - \theta_j$, dashed curves: for $\theta = \xi + \theta_j$ at $\Lambda = 16.07$ μm, $L = 10$ mm and near the optimal non-collinear angle.

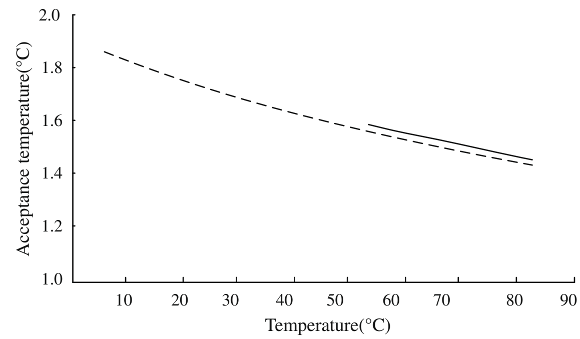


**Fig. 5.** Dependence of acceptance temperature on temperature; solid curve: for $\theta = \xi - \theta_j$ and dashed curve: for $\theta = \xi + \theta_j$; $L = 10$ mm, $\Lambda = 16.07$ μm.

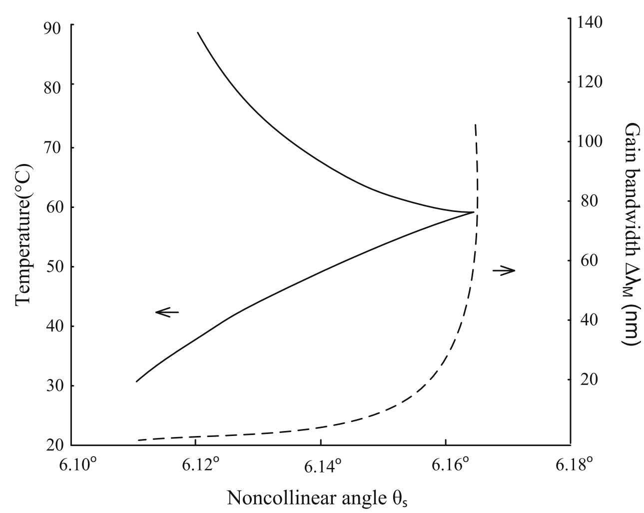


**Fig. 6.** Dependence of gain bandwidth (dashed curve) and crystal temperature (solid curve) on non-collinear angle $\theta_s$ for $\Lambda = 16.07$ μm and $\theta = \xi - \theta_j$ at $L = 10$ mm.

## 5. Spatial–temporal frequency band

We shall analyze the double quasi phase-matched parametric amplification of pulsed light beam in single grating of periodically-poled crystal neglecting the depletion of the pump waves. The corresponding truncated equations of the cascaded non-linear processes are [22,23,27]

$$\frac{\partial A_i}{\partial z} = -\frac{1}{u_i}\frac{\partial A_i}{\partial t} + \frac{i}{2}g_i\frac{\partial^2 A_i}{\partial t^2} - \frac{i}{2k_i}\left(\frac{\partial^2}{\partial x^2} + \frac{\partial^2}{\partial y^2}\right)A_i + i\sigma_i A_p A_s + i\sigma_i A_M^* A_s,$$

$$\frac{\partial A_M}{\partial z} = -\frac{1}{u_M}\frac{\partial A_M}{\partial t} + \frac{i}{2}g_M\frac{\partial^2 A_M}{\partial t^2} - \frac{i}{2k_M}\left(\frac{\partial^2}{\partial x^2} + \frac{\partial^2}{\partial y^2}\right)A_M + i\sigma_M A_s A_i^*, \tag{14}$$

where $A_j$ ($j = i$, $M$ or $p$, $s$) are complex amplitudes of these waves. For simplicity, we assume that pump and signal waves are a quasi-monochromatic and plane one. In the equations $1/u_j = 1/v_j - 1/v_k$ ($j = i$ or $M$, $k = p$ or $s$) is the group velocity mismatch, $g_j$ is the GVD coefficient, $k_j$ is wave vector, $\sigma_j$ is non-linear coupling coefficient and $\sigma_j = 8\pi d_{\mathrm{nm}}\omega_j/c/n_j$. $x$, $y$ are transverse coordinates, $z$ is a longitudinal one, and $t$ is time. We take into consideration the temporal–spatial spectra of idler and mid-infrared waves $f_{i0}$ ($\Delta\omega$, $k_x$, $k_y$) and $f_{M0}$ ($\Delta\omega$, $k_x$, $k_y$). Three-dimensional Fourier transform of Eq. (14) was carried out, we can get [27]

$$\frac{\partial f_i}{\partial z} = -i\Delta_i f_i + i\sigma_i f_p f_s + i\sigma_i f_M f_s,$$

$$\frac{\partial f_M}{\partial z} = -i\Delta_M f_M - i\sigma_M f_s^* f_i, \tag{15}$$

where $f_i = f_{i0}(\Delta\omega, k_x, k_y)$, $f_M = f_{M0}^*(-\Delta\omega, -k_x, -k_y)$ and $\Delta\omega$ is a temporal frequency calculated in respect to central frequencies of the waves and $k_x$ , $k_y$ are spatial frequencies. Here

$$\Delta_i = \frac{\Delta\omega}{u_i} + \frac{g_i}{2}(\Delta\omega)^2 - \frac{(k_x^2 + k_y^2)}{2k_i}.$$

$$\Delta_M = \frac{\Delta\omega}{u_M} - \frac{g_M}{2}(\Delta\omega)^2 + \frac{(k_x^2 + k_y^2)}{2k_M}. \tag{16}$$

Assume that at the input ($z = 0$) of OPA incident pump and signal pulses are, respectively

$$\begin{aligned} A_p(\tau, 0) &= A_p(0)/[\exp(-\tau/T_0) + \exp(\tau/T_0)], \\ A_s(\tau, 0) &= A_s(0)/[\exp(-\tau/T_0) + \exp(\tau/T_0)]. \end{aligned} \tag{17}$$

And at the input the idler and mid-infrared pulses are $A_i(0) = 0$ and $A_M(0) = 0$.

We obtain the solutions of Eq. (15) and temporal–spatial spectra of idler and mid-infrared waves $f_{i0}$ and $f_{M0}$ are, respectively

$$f_{i0} = \frac{\Delta_M \sigma_i f_s f_p}{\Delta}\left[1 + \frac{i}{p}\frac{\Delta}{\Delta_M}\sinh(pz)\exp(+iqz)\right],$$

$$f_{M0} = -\frac{\sigma_i \sigma_M |f_s|^2 f_p}{\Delta}\left[1 - \frac{i}{p}\Delta_M \sinh(pz)\exp(-iqz)\right]. \tag{18}$$

Here

$$p = \sqrt{G^2 - \xi^2},$$

$$\xi = \frac{\Delta_i - \Delta_M}{2} = \left(\frac{1}{u_i} - \frac{1}{u_M}\right)\frac{\Delta\omega}{2} + \frac{g_i + g_M}{4}(\Delta\omega)^2 - \frac{k_x^2 + k_y^2}{4}\left(\frac{1}{k_i} + \frac{1}{k_M}\right),$$

$$\begin{aligned} q &= -\frac{\Delta_i + \Delta_M}{2} \\ &= -\left(\frac{1}{u_i} + \frac{1}{u_M}\right)\frac{\Delta\omega}{2} - \frac{g_i - g_M}{4}(\Delta\omega)^2 + \frac{k_x^2 + k_y^2}{4}\left(\frac{1}{k_i} - \frac{1}{k_M}\right), \end{aligned}$$

$$\Delta = \Delta_M \Delta_i + \sigma_M \sigma_i |f_s|^2 \tag{19}$$

and $G = \sqrt{\sigma_i \sigma_M |f_s|^2}$ is a parametric gain factor for $s + i \to M$ process. The Fourier components of intensity distributions of the output idler and mid-infrared pulses in NDQPM are, respectively.

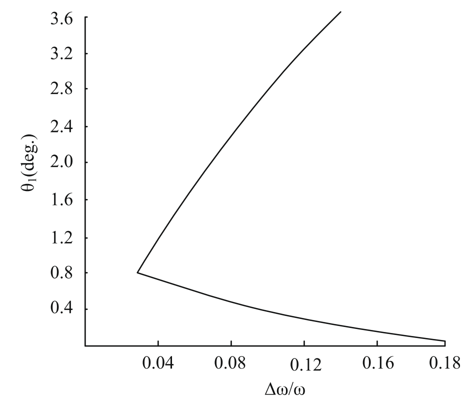


**Fig. 7.** Spatial-temporal frequency band of output idler pulse. $G = 4\,\mathrm{cm}^{-1}$, $L = 10$ mm, $\Lambda = 16.1$ µm, $\lambda_p = 526$ nm, $\lambda_s = 865$ nm and near the optimal non-collinear angle. $\omega$ is central frequency of pulse.

$$I_i = (\sigma_i f_s f_p)^2\left(\frac{\Delta_M}{\Delta}\right)^2\left[1 + \frac{\sinh^2(pz)}{p^2}\left(\frac{\Delta}{\Delta_M}\right)^2 - 2\frac{\Delta}{\Delta_M}\frac{\sinh(pz)}{p}\sin(qz)\right],$$

$$I_M = (\sigma_i f_s f_p)^2\left(\frac{\sigma_M f_s}{\Delta}\right)^2\left[1 + \Delta_M^2\frac{\sinh^2(pz)}{p^2} - 2\frac{\Delta_M}{p}\sinh(pz)\sin(qz)\right]. \tag{20}$$

We assume that a idler beam is angularly dispersed in $y$–$z$ plane ($k_x \approx 0$) and involve into consideration an angle $\theta_1 = k_y/k_i$. In Eq. (19), $(k_x^2 + k_y^2)/4 \approx k_i^2\theta_1^2/4$. Further, we define a STF band at the half-maximum level of spectral intensity $I_i$. A numerically determined STF band of output idler pulse for NDQPM in PPKTP was shown in Fig. 7 for $\Lambda = 16.1$ µm and an optimal non-collinear angle. The STF band is an area under the curves. For the certain $\theta_1$ there exist a corresponding $\Delta\omega_{\max}/\omega$. To make sure that the intensity of output idler pulse is not decreased remarkably, the frequency bandwidth $\Delta\omega < \Delta\omega_{\max}$. For example, when $\theta_1 = 0.4°$, from the figure we obtain $\Delta\omega_{\max}/\omega = 0.1$. Then, the bandwidth ($\Delta v/c$) of temporal frequencies of idler pulse is about $785\,\mathrm{cm}^{-1}$ when pump wavelength is 526 nm and signal wavelength is centered at 865 nm. The certain bandwidth of temporal frequency corresponds to certain tilted angle of the pulse front. Hence, the bandwidth of temporal frequency should match with the tilted angle of the pulse front in a broadband amplification.

## 6. Conclusion

The broadband NDQPM process in single PPKTP crystal to achieve a broad gain bandwidth has been investigated. For PPKTP-NDQPM works at certain signal wavelength pumped at 526 nm, an optimal non-collinear angle exists when the grating period is a corresponding value at fixed temperature in phase-matching condition, where the gain bandwidth reaches the largest and the GVM is zero nearly. By changing the non-collinear angles $\theta_s$, $\theta_p$ near the optimal non-collinear angles, the broadband mid-infrared NDQPM tune can be realized (about $\lambda_M = 2400$–3200 nm). The other optimal phase matching non-collinear angle and grating period can be analyzed with similar method. By tuning the temperature near the optimal grating period and corresponding non-collinear angle, the broadband NDQPM can be also realized. The acceptance angle and acceptance temperature is very small. The gain bandwidth is sensitive to non-collinear angles and temperature, so it is important to control the precision of the non-collinear angle and crystal temperature to keep gain bandwidth.

The coupled equations of NDQPM OPA were discussed and temporal-spatial spectra of output idler and mid-infrared pulses were obtained. The STF band of NDQPM is analyzed. A broadband amplification of angularly dispersed idler requires matching of an angular spectrum of an idler pulse with an acceptance angle of OPA. Certain angular dispersion can significantly increase the amplification of pulsed beam. This analysis is adaptive to different wavelength and other QPM materials. These theoretical results are very useful for designing broadband NDQPM OPA system.

## References


[1] W.Q. Zhang, Appl. Opt. 45 (20) (2006) 4977.
[2] A. Fragemann, V. Pasiskevicius, F. Laurell, Opt. Lett. 30 (17) (2005) 2296.
[3] V. Smilgevičus, A. Stabinis, A. Piskarskas, V. Pasiškevičius, J. Hellström, S. Wang, F. Laurell, Opt. Commun. 173 (2000) 365.
[4] I. Jovanovic, Jason R. Schmidt, C.A. Ebbers, Appl. Phys. Lett. 83 (2003) 4125.
[5] M. Thhonen, V. Pasiskevicius, A. Fragemann, C. Canalias, F. Laurell, Appl. Phys. B 85 (2006) 73.
[6] L. Cardoso, G. Figueira, Opt. Commun. 251 (2005) 405.
[7] Hongjun Liu, Zhao Wei, Hongying Wang, Xiaoli Li, Yishan Wang, Opt. Commun. 261 (2006) 163.
[8] C. Wang, Y.X. Leng, X. Liang, B. Zhao, Z. Xu, Opt. Commun. 246 (2005) 323.
[9] Da Wun Chen, J. Opt. Soc. Am. B 20 (7) (2003) 1527.
[10] M. Tiihonen, V. Pasiskevicius, F. Laurell, Opt. Express 14 (19) (2006) 8728.
[11] David Artigas, Derryck T. Reid, Opt. Commun. 210 (2002) 113.
[12] Karl A. Tillman, Derryck T. Reid, J. Opt. Am. B 21 (8) (2004) 1551.
[13] W.Q. Zhang, Opt. Commun. 252 (2005) 179.
[14] O. Pfister, J.S. Wells, L. Hollberg, L. Zink, D.A. Vanbaak, M.D. Levenson, W.R. Bosenberg, Opt. Lett. 22 (1997) 1211.
[15] K. Fradkin-Kashi, A. Arie, P. Urenski, G. Rosenman, Phys. Rev. Lett. 88 (2002) 023903.
[16] S.M. Saltiel, A.A. Sukhorukov, Y.S. Kivishar, Prog. Opt. 47 (2005) 1.
[17] W.Q. Zhang, F. Yang, X.Y. Li, Opt. Commun. 282 (2009) 1406.
[18] A. Stabinis, J. Krupic, Opt. Commun. 271 (2007) 564.
[19] W.Q. Zhang, Opt. Commun. 105 (1994) 226.
[20] K. Kato, E. Takaoka, Appl. Opt. 41 (2002) 5040.
[21] R.A. Baumgarther, R.L. Byer, IEEE J. Quantum Electron QE-15 (1979) 432.
[22] Y.Q. Qin, Y.Y. Zhu, C. Zhang, N.B. Ming, J. Opt. Soc. Am, B 20 (1) (2003) 73.
[23] Wei Quan Zhang, Opt. Commun. 274 (2007) 451.
[24] W.Q. Zhang, Optik (Stuttgart) 104 (3) (1997) 87.
[25] Shai Emanuel, Ady Arie, Appl. Opt. 42 (33) (2003) 6661.
[26] B.Z. Zhao, X.Y. Liang, Y.X. Leng, C. Wang, Z.Z. Xu, Opt. Commun. 248 (2005) 387.
[27] R. Butkus, S. Orlov, A. Piskarskas, V. Smilgevičius, A. Stabinis, Opt. Commun. 227 (2003) 237.